PROCEEDINGS OF SCIENCE

Perturbative calculation of Z_q at the one-loop level using HYP-smeared staggered quarks

Benjamin J. Choi*, Weonjong Lee
Lattice Gauge Theory Research Center, CTP, and FPRD,
Department of Physics and Astronomy, Seoul National University, Seoul 08826, South Korea
E-mail: benjaminchoi@snu.ac.kr, wlee@snu.ac.kr

Jangho Kim
Institut für Theoretische Physik, Johann Wolfgang Goethe-Universität,
Max-von-Laue-Str. 1, 60438 Frankfurt am Main, Germany
E-mail: jkim@th.physik.uni-frankfurt.de

Sungwoo Park
Los Alamos National Laboratory, Theoretical Division, T-2, Los Alamos, NM 87545, USA
E-mail: kunsung5@gmail.com

Stephen R. Sharpe
Department of Physics, University of Washington, Seattle, WA 98195-1560, USA
E-mail: srsharpe@uw.edu

SWME Collaboration

We present matching factors for Z_q calculated perturbatively at the one-loop level with improved staggered quarks. We calculate Z_q with HYP-smeared staggered quarks and Symanzik-improved gluons using both RI-MOM and RI′-MOM schemes. We compare the results with those obtained using the nonperturbative renormalization (NPR) method.

The 36th Annual International Symposium on Lattice Field Theory - LATTICE2018
22-28 July, 2018
Michigan State University, East Lansing, Michigan, USA.

*Speaker.

© Copyright owned by the author(s) under the terms of the Creative Commons Attribution-NonCommercial-NoDerivatives 4.0 International License (CC BY-NC-ND 4.0).

PoS(LATTICE2018)295

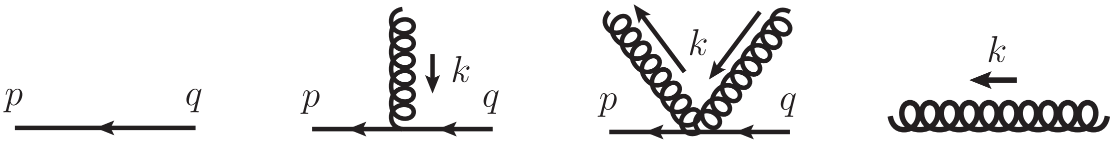

(a) quark propagator (b) one-gluon vertex (c) two-gluon vertex (d) gluon propagator

Figure 1: Feynman rules at the one-loop level

1. Introduction

In order to convert the results for matrix elements from lattice QCD into those in a continuum scheme, we need to calculate the corresponding renormalization factors. This can be done either using perturbation theory (PT) or with a non-perturbative method such as non-perturbative renormalization (NPR). The former suffers from truncation errors, while the latter has the usual systematic errors associated with lattice quantities, as well as the need for a window in which $\Lambda_{\text{QCD}} \ll \mu \ll 1/a$, where μ is the renormalization scale. Although NPR is generally preferred, it is useful to make detailed comparisons with PT, in particular since some lattice calculations of matrix elements use perturbative matching. Here we present such a comparison for the Z_q, the quark field renormalization, which is an ingredient in NPR calculations for almost all operators. Specifically, we compare one-loop results for the asqtad action and HYP-smeared staggered valence quarks with those obtained using NPR on the MILC "coarse" ensemble ($a \approx 0.12\,\text{fm}$).

2. Feynman rules

The free propagator for HYP staggered quarks in Fig. 1a is (with color factors excluded)

$$S_0(p,-q) = \bar{\delta}\left(p'-q'\right) \frac{\dfrac{i}{a}\sum\limits_{\mu} \sin\left(ap'_\mu\right) \overline{\overline{(\gamma_\mu \otimes \mathbf{1})}}_{AB} + m_0 \overline{\overline{(\mathbf{1}\otimes\mathbf{1})}}_{AB}}{\sum\limits_{\alpha} \dfrac{1}{a^2} \sin^2\left(ap'_\alpha\right) + m_0^2} \tag{2.1}$$

where $p = p' + \dfrac{\pi}{a}A$, and $q = q' + \dfrac{\pi}{a}B$. Here, $p'_\mu, q'_\nu \in \left(-\dfrac{\pi}{2a}, +\dfrac{\pi}{2a}\right]$ are momenta defined in the reduced Brillouin zone [1], $\bar{\delta}\left(p'-q'\right)$ is the periodic delta function which is nonzero for $q'_\mu = p'_\mu$ (mod $\dfrac{2\pi}{a}$), and A and B are hypercubic vectors: $A_\mu, B_\nu \in \{0,1\}$. The spin-taste factors $\overline{\overline{(\gamma_S \otimes \xi_F)}}_{AB}$ are explained in Ref. [1].

The HYP action uses HYP-smeared links, V_μ, which must be expressed in terms of the original thin links U_μ. To do so we expand both links as

$$U_\mu(x) = \exp\left[iagA_\mu\left(x + \frac{a}{2}\hat{\mu}\right)\right], \qquad V_\mu(x) = \exp\left[iagB_\mu\left(x + \frac{a}{2}\hat{\mu}\right)\right], \tag{2.2}$$

where $A_\mu(x) = \sum\limits_a A^a_\mu(x) T^a$ is the gluon field, while $B_\mu(x) = \sum\limits_a B^a_\mu(x) T^a$ is smeared gauge field. The latter can be written as a perturbative expansion in powers of $A_\mu(x)$'s

$$B_\mu(x) = \sum_{n=1}^{\infty} B^{(n)}_\mu(x) = B^{(1)}_\mu(x) + B^{(2)}_\mu(x) + B^{(3)}_\mu(x) + \ldots, \tag{2.3}$$

PoS(LATTICE2018)295

where $B_\mu^{(n)}$ stands for a term of order $(A_\mu)^n$. Only the linear term, $B_\mu^{(1)}(x)$, contributes to the renormalization at the one-loop level [1, 2]. The relation between $B_\mu^{(1)}(x)$ and $A_\mu(x)$ is

$$B_\mu^{(1)}(x) = \int_{-\pi/a}^{\pi/a} \frac{d^4k}{(2\pi)^4} \sum_\nu h_{\mu\nu}(k)\tilde{A}_\nu(k)e^{ik\cdot x}, \qquad A_\mu(x) = \int_{-\pi/a}^{\pi/a} \frac{d^4k}{(2\pi)^4} \tilde{A}_\mu(k)e^{ik\cdot x}, \tag{2.4}$$

where $h_{\mu\nu}(k)$ is the smearing kernel which describes details of the blocking transformation for the fat link.

$$h_{\mu\nu}(k) = \delta_{\mu\nu}D_\mu(k) + (1-\delta_{\mu\nu})\tilde{G}_{\nu,\mu}(k)\bar{s}_\mu\bar{s}_\nu \tag{2.5}$$

$$D_\mu(k) = 1 - d_1\sum_{\nu\neq\mu}\bar{s}_\nu^2 + d_2\sum_{\substack{\nu<\rho\\ \nu,\rho\neq\mu}}\bar{s}_\nu^2\bar{s}_\rho^2 - d_3\bar{s}_\nu^2\bar{s}_\rho^2\bar{s}_\sigma^2 + d_4\sum_{\nu\neq\mu}\bar{s}_\nu^4 \tag{2.6}$$

$$\tilde{G}_{\nu,\mu}(k) = d_1 - d_2\frac{\bar{s}_\rho^2+\bar{s}_\sigma^2}{2} + d_3\frac{\bar{s}_\rho^2\bar{s}_\sigma^2}{3} + d_4\bar{s}_\nu^2. \tag{2.7}$$

Here, $\mu\neq\nu\neq\rho\neq\sigma$ and $\bar{s}_\mu = \sin(ak_\mu/2)$. In order to remove $\mathscr{O}(a^2)$ taste symmetry breaking interactions at tree level, we choose the parameters to be [3]

$$d_1 = 1, \quad d_2 = 1, \quad d_3 = 1, \quad d_4 = 0. \tag{2.8}$$

The Feynman rule for the one-gluon emission vertex of Fig. 1b is

$$V^I_{\mu;\alpha}(p,-q,k) = -igT^I\cos\left(\frac{ak_\mu}{2} - aq'_\mu\right)h_{\mu\alpha}(k)\overline{\overline{(\gamma_\mu\otimes\mathbf{1})}}_{AB}\bar{\delta}(p'-q'+k), \tag{2.9}$$

where T^I is the SU(3) color generator, while that for the two-gluon emission vertex of Fig. 1c is

$$V_{\mu\nu;\alpha\beta}(p,-q,k) = -iag^2C_F\delta_{\mu\nu}\sin(aq'_\mu)h_{\mu\alpha}(k)h_{\mu\beta}(k)\overline{\overline{(\gamma_\mu\otimes\mathbf{1})}}_{AB}\bar{\delta}(p'-q'), \tag{2.10}$$

where $C_F = \sum_I (T^I)^2 = 4/3$.

The MILC asqtad ensembles use a Symanzik-improved gluon action. The corresponding gluon propagator can be written as [4]

$$\mathscr{D}^{\text{Imp.}}_{\mu\nu}(k) = (1-\alpha)\frac{\mathscr{P}_{\mu\nu}}{\hat{k}^2} + \frac{\left[\hat{k}^2(\hat{k}^2-\tilde{c}x_1)+\tilde{c}^2x_2\right]\delta^T_{\mu\nu} + \tilde{c}(\hat{k}^2-\tilde{c}x_1)\mathscr{M}_{\mu\nu} + \tilde{c}^2\left[\mathscr{M}^2\right]_{\mu\nu}}{f\left\{\hat{k}^2\left[\hat{k}^2(\hat{k}^2-\tilde{c}x_1)+\tilde{c}^2x_2\right]-\tilde{c}^3x_3\right\}}, \tag{2.11}$$

where $\alpha = 0(1)$ for Feynman (Landau) gauge. The notation in this result is explained in Ref. [4]. Although the gluon action used in generating the MILC lattices includes improvements beyond tree level, for our one-loop perturbative calculation it is appropriate to use the tree-level Symanzik improvement coefficients, with the redundant coefficient chosen according to the the convention of Ref. [5]. This choice fixes the constants in Eq. (2.11).

3. Staggered quark self energy

Using the Feynman rules given above, we can express the one-loop quark self-energy as

$$\Sigma(p,-q) = \int_{-\pi/a}^{\pi/a}\frac{d^4kd^4\ell_1d^4\ell_2}{(2\pi)^{12}}\sum_{\substack{\mu,\nu,\\ \alpha,\beta}}\sum_I V^I_{\mu;\alpha}(p,-\ell_1,-k)S_0(\ell_1,-\ell_2)V^I_{\nu;\beta}(-q,\ell_2,k)\mathscr{D}^{\text{Imp.}}_{\alpha\beta}(k)$$

PoS(LATTICE2018)295

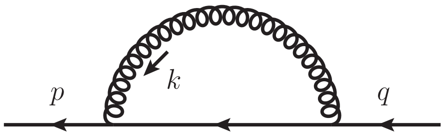

(a) Sunset diagram

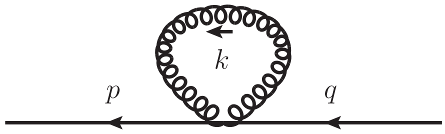

(b) Tadpole diagram

Figure 2: Feynman diagrams for quark self energy at the one-loop level

$$+\frac{1}{2}\int_{-\pi/a}^{\pi/a}\frac{d^4k}{(2\pi)^4}\sum_{\substack{\mu,\nu,\\ \alpha,\beta}} V_{\mu\nu;\alpha\beta}(p,-q,k)\,\mathscr{D}^{\text{Imp.}}_{\alpha\beta}(k) \tag{3.1}$$

$$=\Sigma(p')\,\bar{\delta}(p'-q')\,. \tag{3.2}$$

In Eq. (3.1), the first term corresponds to Fig. 2a and the second to Fig. 2b.

We use the technical tools in Ref. [6] to calculate the integrals in Eq. (3.1). If we choose the momentum p' so that $|ap'_\mu| \ll 1$, we can rewrite the self energy as

$$\Sigma(p') = -i\Sigma_1 p'_\mu \overline{\overline{(\gamma_\mu\otimes\mathbf{1})}}_{AB} + m_0\Sigma_2\overline{\overline{(\mathbf{1}\otimes\mathbf{1})}}_{AB} + \mathscr{O}(a^2) \tag{3.3}$$

where

$$\Sigma_1(p') = \frac{g^2C_F}{(4\pi)^2}\Bigg[(1-\alpha)\left\{\log\left[a^2\left(m_0^2+p'^2\right)\right] + \frac{m_0^2}{p'^2}\left(1-\frac{m_0^2}{p'^2}\log\left[1+\frac{p'^2}{m_0^2}\right]\right)\right\}$$
$$-(1-\alpha)(F_{0000}-\gamma_E+1)+Z+ZT-\frac{3}{2}+\mathscr{O}(a)\Bigg], \tag{3.4}$$

$$\Sigma_2(p') = \frac{g^2C_F}{(4\pi)^2}\Bigg[(4-\alpha)\left\{\log\left[a^2\left(m_0^2+p'^2\right)\right] - \left(1-\frac{m_0^2}{p'^2}\log\left[1+\frac{p'^2}{m_0^2}\right]\right)\right\}$$
$$-(4-\alpha)(F_{0000}-\gamma_E+1)+ZM+\mathscr{O}(a)\Bigg]. \tag{3.5}$$

Here, $Z+ZT = 0.7737683(12)$, $ZM = 13.242431(11)$, and $F_{0000}-\gamma_E+1 = 4.7920095689746(13)$ are numerical results for the Feynman diagrams obtained using the VEGAS algorithm [7].

The inverse quark propagator S^{-1} can now be expressed as

$$S^{-1} = S_0^{-1} - \Sigma(p') = -i(1-\Sigma_1)p'_\mu\overline{\overline{(\gamma_\mu\otimes\mathbf{1})}}_{AB} + (1-\Sigma_2)m_0\overline{\overline{(\mathbf{1}\otimes\mathbf{1})}}_{AB}\,. \tag{3.6}$$

As usual, this form holds to all orders in perturbation theory, although here we use only the one loop form of $\Sigma_{1,2}$.

4. Results for Z_q in the RI-MOM scheme

Using the Ward identity following from the conservation of the vector current (which holds also with staggered fermions) one can derive the following identity for Z_q in the RI-MOM scheme [8]:

$$Z_q = \frac{1}{48}\mathrm{tr}\left(\frac{i}{4}\sum_\rho\overline{\overline{(\gamma_\rho\otimes\mathbf{1})}}\frac{\partial}{\partial p'_\rho}S^{-1}(p')\right)\Bigg|_{p'^2=\mu^2}\,. \tag{4.1}$$

PoS(LATTICE2018)295

Substituting Eq. (3.6) into this result we find

$$Z_q = \left(1 - \Sigma_1(p') - \frac{1}{4} \sum_\rho p'_\rho \frac{\partial \Sigma_1(p')}{\partial p'_\rho} \right) \Bigg|_{p'^2=\mu^2} . \tag{4.2}$$

Similarly, implementing the RI$'$-MOM scheme of Ref. [8] (as has been done with staggered fermions in Ref. [9]) we find

$$Z'_q = \left(1 - \Sigma_1(p')\right) \Big|_{p'^2=\mu^2} . \tag{4.3}$$

The result differs only in the absence of the last term in Eq. (4.2).

Combining results for Σ_1 in Eq. (3.4) in the chiral limit ($m_0 = 0$) with the master formulae Eqs. (4.2) and (4.3) we obtain the one-loop results for Z_q and Z'_q:

$$Z_q(\mu) = 1 - \frac{g^2 C_F}{(4\pi)^2} \left[Z + ZT - \frac{3}{2} + (1-\alpha)\left(\log\left[a^2\mu^2\right] + \frac{1}{2} - X \right) + \mathcal{O}(a) \right] , \tag{4.4}$$

$$Z'_q(\mu) = 1 - \frac{g^2 C_F}{(4\pi)^2} \left[Z + ZT - \frac{3}{2} + (1-\alpha)\left(\log\left[a^2\mu^2\right] - X \right) + \mathcal{O}(a) \right] , \tag{4.5}$$

where $X \equiv F_{0000} - \gamma_E + 1$.

To evaluate Z_q and Z'_q for scales μ far from $1/a$, we use the horizontal matching method of Refs. [10, 11]. We first set $\mu = 1/a$ in the one-loop results, and then evolve Z_q from $\mu = 1/a$ to the final scale μ_0 with four-loop running, using the results from Ref. [12]. Typically we use $\mu_0 = 2\text{GeV}$ or 3GeV. The result is

$$Z_q(\mu_0) = \frac{c(\mu_0)}{c(\mu)} Z_q(\mu = 1/a) , \qquad Z'_q(\mu_0) = \frac{c'(\mu_0)}{c'(\mu)} Z'_q(\mu = 1/a) , \tag{4.6}$$

where the prefactors $c(\mu_0)/c(\mu)$ and $c'(\mu_0)/c'(\mu)$ are the four-loop RG running factors in the RI-MOM and RI$'$-MOM schemes, respectively.

When using these formulae to give numerical values for Z_q and Z'_q we estimate the systematic error due to truncating the perturbative series at one loop by assuming an $\mathcal{O}(1)$ coefficient of the missing α_s^2 term. Specifically, following Ref. [13], we estimate the truncation error to be

$$E^{(\prime)}_{\text{trunc.}} \approx Z^{(\prime)}_q \times \alpha_s^2(\mu = 1/a) . \tag{4.7}$$

Specifically, we use $\alpha_s(\mu = 1/a)$ in the $\overline{\text{MS}}$ scheme, evaluated from the PDG value for $\alpha_s(M_Z)$ using four-loop running.

5. Numerical results for Z_q

In Fig. 3, we present results for Z_q and Z'_q, evaluated in perturbation theory in Landau gauge, at three scales: $\mu_0 = 1/a$ (blue circles), $\mu_0 = 2\text{GeV}$ (green circles) and $\mu_0 = 3\text{GeV}$ (red circles), using Eq. (4.6). In Table 1a, we give the corresponding numerical values.

We now compare the results with those obtained using nonperturbatively. We have results for Z_q in the RI-MOM scheme using NPR with HYP-smeared staggered fermions on the MILC

PoS(LATTICE2018)295

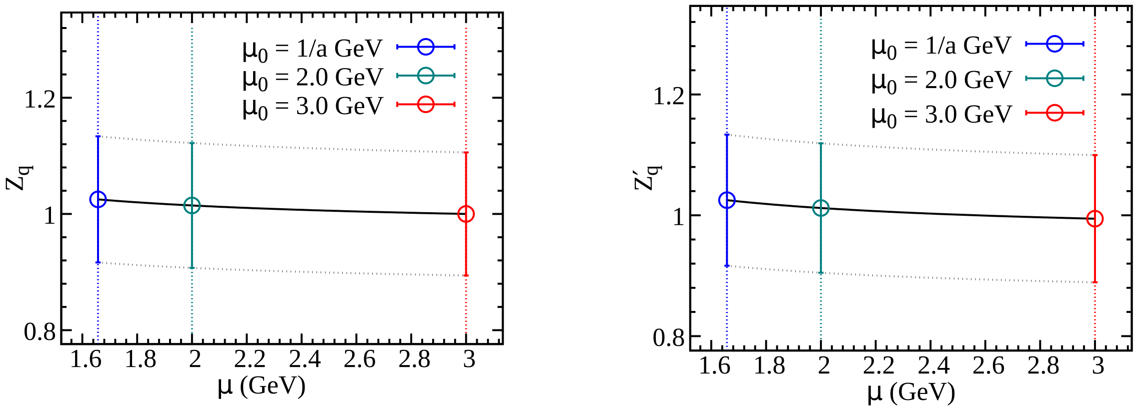

(a) Z_q (b) Z'_q

Figure 3: One loop perturbative results for Z_q and Z'_q in Landau gauge.

	Landau Gauge		Feynman Gauge	
	$\mu_0 = 2$GeV	$\mu_0 = 3$GeV	$\mu_0 = 2$GeV	$\mu_0 = 3$GeV
Z_q	1.02(11)	1.00(11)	1.14(12)	1.09(12)
Z'_q	1.01(11)	0.99(11)	1.15(12)	1.09(12)

(a) One-loop perturbation theory

Z_q	NPR (Landau gauge)	
	$\mu_0 = 2$GeV	$\mu_0 = 3$GeV
$\gamma_\mu \otimes \mathbf{1}$	1.0548(59)(229)	1.0392(58)(226)
$\gamma_{\mu 5} \otimes \xi_5$	1.0319(61)(229)	1.0166(61)(226)

(b) NPR

Table 1: Results on Z_q and Z'_q at $\mu_0 = 2$GeV and 3GeV.

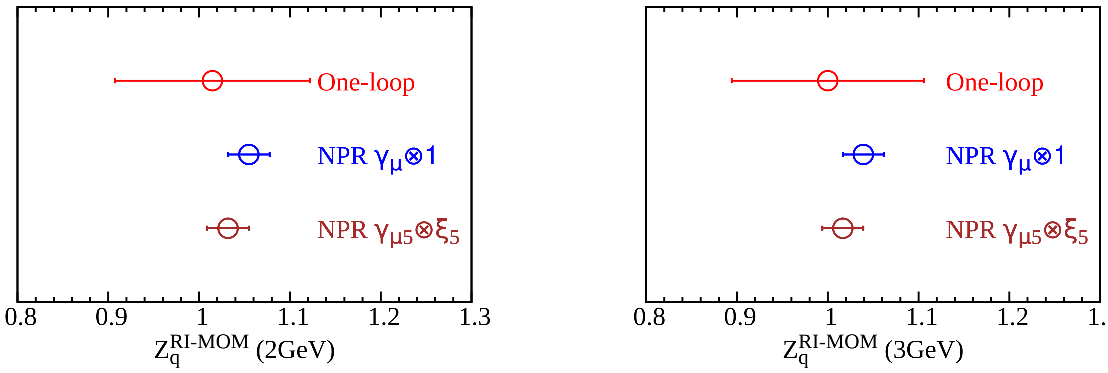

(a) $\mu_0 = 2$GeV (b) $\mu_0 = 3$GeV

Figure 4: Comparison of results for $Z_q(\mu_0)$ between one-loop perturbation theory and NPR.

asqtad coarse lattice ensemble 2064f21b676m010m050, for which $1/a = 1.657(2)$GeV [14, 15]. We present these results in Table 1b. Here, NPR $\gamma_\mu \otimes \mathbf{1}$ ($\gamma_{\mu 5} \otimes \xi_5$) indicates results for Z_q obtained using the conserved vector (axial) current. The errors are, respectively, statistical and systematic.

A graphical comparison is shown in Fig. 4. We find that all the results are consistent within the quoted uncertainties, with the results from NPR being significantly more accurate.

Acknowledgments

W. Lee would like to acknowledge the support from the KISTI supercomputing center through

PoS(LATTICE2018)295

the strategic support program for the supercomputing application research (No. KSC-2016-C3-0072). The research of W. Lee is supported by the Creative Research Initiatives Program (No. 2017013332) of the NRF grant funded by the Korean government (MEST). The work of S. Sharpe was supported in part by the US DOE grants no. DE-FG02-96ER40956 and DE-SC0011637. Computations were carried out in part on the DAVID GPU clusters at Seoul National University.

References

[1] A. Patel and S. R. Sharpe *Nucl.Phys.* **B395** (1993) 701–732, [hep-lat/9210039].

[2] W. Lee *Phys. Rev.* **D66** (2002) 114504, [hep-lat/0208032].

[3] W. Lee and S. R. Sharpe *Phys.Rev.* **D66** (2002) 114501, [hep-lat/0208018].

[4] J. Kim, W. Lee, and S. R. Sharpe *Phys. Rev.* **D81** (2010) 114503, [1004.4039].

[5] M. Luscher and P. Weisz *Commun. Math. Phys.* **97** (1985) 59. [Erratum: Commun. Math. Phys.98,433(1985)].

[6] M. F. L. Golterman and J. Smit *Nucl. Phys.* **B245** (1984) 61.

[7] G. P. Lepage *J. Comput. Phys.* **27** (1978) 192.

[8] G. Martinelli *et al. Nucl. Phys.* **B445** (1995) 81–108, [hep-lat/9411010].

[9] A. T. Lytle and S. R. Sharpe *Phys. Rev.* **D88** (2013), no. 5 054506, [1306.3881].

[10] R. Gupta *et al. Phys. Rev.* **D55** (1997) 4036–4054, [hep-lat/9611023].

[11] T. Bae *et al. Phys. Rev.* **D82** (2010) 114509, [1008.5179].

[12] K. Chetyrkin and A. Retey *Nucl.Phys.* **B583** (2000) 3–34, [hep-ph/9910332].

[13] **SWME** Collaboration, T. Bae *et al. Phys. Rev. Lett.* **109** (2012) 041601, [1111.5698].

[14] J. Kim, B. Yoon, and W. Lee *PoS* **LATTICE2012** (2012) 241, [1211.2077].

[15] J. Kim, J. Kim, W. Lee, and B. Yoon *PoS* **LATTICE2013** (2014) 308, [1310.4269].

PoS(LATTICE2018)295